View metadata, citation and similar papers at core.ac.uk
brought to you by CORE
provided by The University of Utah: J. Willard Marriott Digital Library

Organic Spin-Valves: Physics and Applications

Z. Valy Vardeny, Z. H. Xiong, Di Wu, Fujian Wang, and Jing Shi

Physics Department, University of Utah
Salt Lake City, Utah, 84112, USA

Abstract. Spin-valve devices of organic semiconductors in the vertical configuration using a variety of exotic and regular ferromagnetic electrodes were fabricated and studied as a function of applied magnetic field, temperature and applied bias voltage. These devices show that spin polarized carriers can be injected from ferromagnetic electrodes into organic semiconductors and diffuse without loss of spin polarization for distances of the order of 100 nm at low temperatures.

Keywords: Organic semiconductors, spin-valves, spin polarized carrier injection, spin-polarized transport.
PACS: 75.25.Dc; 72.25.Hg; 72.25.Rb; 72.80.Le.

INTRODUCTION

The discoveries of giant magnetoresistance (GMR), colossal magnetoresistance, and tunneling magnetoresistance have not only generated a great deal of excitement in condensed matter physics and materials sciences, but also found their applications in magnetic recording and memory technologies [1–3]. Spin-valve read heads and magnetic tunnel junction based random access memory devices are two examples of such applications. For both high-density recording and high-density non-volatile memory, incorporating semiconductor materials into the existing spintronic devices is highly desirable, since it would transform the usually passive devices into active devices. Semiconductor Spintronics can offer many other potential applications in information processing, transmission and storage [4, 5]. But to realize these potentials, efficient means of injecting spin-polarized charges from metallic or semimetallic electrodes into semiconductors must first be demonstrated. Spin injection from ferromagnetic (FM) metals into nonmagnetic metals has been well studied and documented [2, 3]. However spin injection by electrical means from FM into semiconductors remains a challenge.

Schmidt et al. [6] have pointed out that the basic obstacle for spin injection from a FM into a semiconductor originates from the conductance mismatch between the two materials. Recently Rashba [7], Smith and Silver [8] and Albrecht and Smith [9] have shown that the conductance mismatch problem could be circumvented if the injection occurs via tunneling. Since charge injection from metallic electrodes into organic semiconductors (OSEC) occurs mainly through tunneling [10], OSEC seem to be promising alternatives for semiconductor Spintronics [11]. In addition to efficient spin-polarized injection, a long spin relaxation time is also needed for spin transport applications in the transport layer. The building block atoms of OSEC are light (i.e. having low atomic number Z) with very small spin-orbit coupling. Moreover the π-electron wave function has zero amplitude on the nucleus sites, thereby minimizing the

CP786, *Electronic Properties of Novel Nanostructures,* edited by H. Kuzmany, J. Fink, M. Mehring, and S. Roth
© 2005 American Institute of Physics 0-7354-0275-2/05/$22.50

effect of hyperfine interaction. These unique properties show that OSEC may be rather effective for molecular Spintronics applications. In addition, OSEC have the potential to bring novel functionalities that do not exist in inorganic spintronic devices. One such functionality is the very efficient light emitting capability of OSEC. Here we review our recent work [12] where we demonstrated the first organic semiconductor spin-valve based on the small molecule tris-(8-hydroxyquinoline) aluminum (Alq_3).

DEVICE FABRICATION AND MEASUREMENTS

A vertical spin-valve device consists of three layers, two ferromagnetic electrodes (FM1 and FM2) and a non-magnetic spacer (Fig. 1a). By engineering the FM electrodes to have different coercive fields, the magnetizations in FM1 and FM2 can have either parallel or anti-parallel alignment in different magnetic field ranges. We have chosen Alq_3 as our OSEC spacer material in the spin-valves, since it can be easily evaporated and integrated with other electrode materials. The bottom ferromagnetic electrode (FM1) was a 100 nm-thick $La_{1/3}Sr_{2/3}O_3$ (LSMO) film, grown epitaxially on a $LaAlO_3$ substrate. LSMO is believed to be a half-metallic ferromagnet that possesses near 100% spin polarization [13] (For a recent review of colossal magnetoresistance see Ref. [14]). Unlike metallic films, the LSMO films are already stable against oxidation. In fact, our LSMO films were cleaned and reused multiple times without any degradation. The OSEC film (Alq_3) was then thermally evaporated onto the LSMO film, followed by Co film (FM2) evaporation in the same vacuum chamber, using a shadow mask. The active device size was about 2x3 mm^2. The OSEC film thickness ranged from 130 nm to 260 nm (Fig. 1b). The magneto-resistance (MR) of the obtained spin-valve device was measured in a close-cycled refrigerator from 11 to 300 K by sending a constant current through it via the two interfaces, while varying an external in-plane magnetic field, H (Fig. 1c). The hysteresis loops of the magnetization vs. H for the FM electrodes were measured by the magneto-optic Kerr effect (MOKE) over the same temperature range.

A schematic band diagram of a typical LSMO/Alq_3/Co device is shown in Fig. 1c. In the rigid band approximation, namely without taking into account the relaxation and polarization energy associated with charge injection, the highest occupied molecular orbital (HOMO) of Alq_3 lies about 0.9 eV below the Fermi levels, E_F of the FM electrodes, whereas the lowest unoccupied molecular orbital (LUMO) lies about 2.00 eV above E_F. At low applied bias voltages, V, holes are injected from the anode into the HOMO level of the OSE mainly by tunnelling through the bottom potential barrier. In addition, the similar work function value, ϕ of the two electrodes (Fig. 1c) leads to a symmetric I-V response (Fig. 1d). For fabricated devices with $d > 100$ nm we found that the I-V characteristic was non-linear with a weak temperature dependence (Fig. 1d), indicative of carrier injection by tunnelling. Control devices with similar OSE thickness, in which ITO replaced the LSMO bottom electrode, showed electro-luminescence (EL) and also a conductivity detected magnetic resonance at $g \approx 2$, indicating carrier injection into the OSE. In addition, at low bias voltages we measured a typical resistance of 10^4-10^5 Ω that depends on the deposition rate and thickness of the Co electrode; such resistance is also consistent with a dominant pinhole-free organic spacer. Devices with $d < 100$ nm, however showed a linear I-V response and lack of EL, leading us to believe that theses devices have an 'ill-defined' layer of up to 100 nm that may contain pinholes

and Co inclusions. These findings suggest that the OSE spacers in the spin-valve devices fabricated with d >100 nm may be composed of two sub-layers: one sub-layer with a thickness d_0 ~ 100 nm thick immediately below the Co electrode that contains Co inclusions due to the inter-diffusion; and a second sub-layer of neatly deposited Alq_3 between this defected sub-layer and the LSMO film having a thickness $d-d_0$, in which carrier transport is dominated by carrier drift.

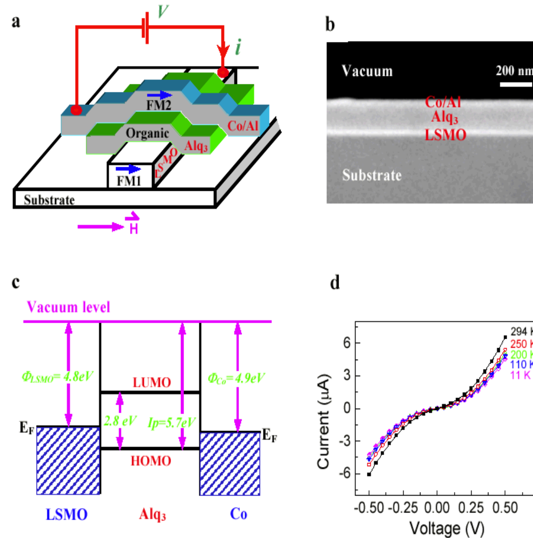

FIGURE 1. The structure and transport properties of the fabricated organic spin-valve devices. **a,** Schematic representation of a typical device that consists of two FM electrodes (FM_1 and FM_2) and an OSE spacer. Spin-polarized electrical current, I flows from FM_1 (LSMO), through the OSE spacer (Alq_3), to FM_2 (Co) when a positive bias, V is applied. **b,** Scanning electron micrograph of a functional organic spin valve consisting of 60-monolayer thick LSMO film, 160 nm Alq_3 spacer, 3.5 nm Co and 35 nm thick Al electrode. **c,** Schematic band diagram of the OSE device showing the Fermi levels and the work functions of the two FM electrodes, LSMO and Co, respectively, and the HOMO-LUMO levels of Alq_3. **d,** I-V response of the organic spin-valve device with d = 200 nm at several temperatures.

RESULTS AND DISCUSSION

Fig. 2a shows a typical magnetoresistance loop obtained in an LSMO/Alq_3/Co spin-valve device with d = 130 nm; the magnetoresistance curves of three other devices having larger d were also measured and their figure of merit $\Delta R/R$ is summarized in Fig. 2b. A sizeable $\Delta R/R$ of 40%, which is a giant magnetoresistance (GMR) response comparable to that obtained in metallic GMR spin-valves, is observed at 11 K. The GMR of the devices with larger d is progressively smaller, but still measurable up to d = 250 nm (Fig.

2b). MOKE measurements performed on the LSMO bottom electrode of the device in Fig. 1a indicate that the coercive field of the LSMO film is $H_{c1} \approx 30$ Oe at 11 K. Whereas the top Co electrode of this device is not accessible to MOKE due to the Al top contact, nevertheless the coercive field of a Co film of the same thickness deposited on Alq_3 under similar conditions was measured to be $H_{c2} \approx 150$ Oe at 11 K; much greater than that of the LSMO. Clearly then, the magnetization orientations in the two FM electrodes are anti-parallel to each other when the external field H is between H_{c1} and H_{c2}; in contrast, the magnetization orientations are parallel to each other when the field strength $H > H_{c2}$. Therefore, the observed GMR hysteresis is undoubtedly due to the spin-valve effect. We note that the resistance in the anti-parallel alignment is lower than that in the parallel alignment, which is opposite to the spin-valve effect usually obtained using two identical FM electrodes, or two different "d-band" metallic FM electrodes in some devices. This "inverse magnetoresistance" was also previously seen in $LSMO/SrTiO_3/Co$ and $LSMO/Ce_{0.69}La_{0.31}O_{1.845}/Co$ magnetic tunnel junction devices having extremely thin insulating spacers (~2 nm).

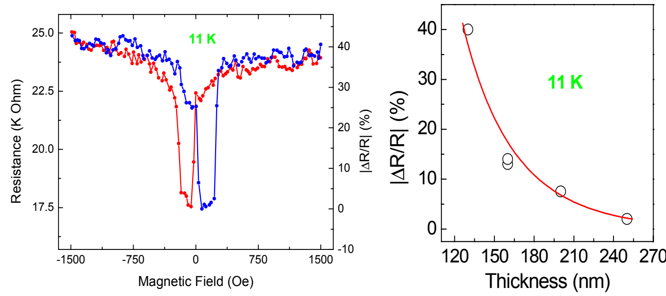

FIGURE 2. **(a)** The MR response of a $LSMO/Alq_3/Co$ spin-valve at 11K showing a GMR response of ~ 40%. The blue (red) curve was measured in the forward (backward) magnetic field sweep direction. **(b)** The spin-valve figure of merit $\Delta R/R$ of spin-valves fabricated on the same LSMO film but with different Alq_3 OSEC layer thickness. The line through the data points is a theoretical fit as explained in the text.

We analyzed the obtained GMR effect and its dependence on d using a simple injection and diffusion model [12]. In the present organic spin-valves, the neatly deposited OSE sub-layer with thickness $(d-d_0)$ is actually so thick (>30 nm) that simple quantum mechanical tunneling through it is not a viable possibility. Although the detailed physical picture is lacking at the moment, nevertheless we assume that there exists a potential barrier for spin injection at the Co/OSE interface (Fig. 1c), which may be self-adjusted [11]. Once carriers are injected through this interface they easily reach the neat sub-layer, where they drift under the influence of the electric field toward the other interface from which they can be extracted. As the injected carriers reach the end of the ill-defined sub-layer, the spin polarization is p_1; it further decays in the remaining neatly deposited sub-layer with a surviving probability $\exp[-(z-d_0)/\lambda_S]$, where z is the drift/diffusion distance along the normal direction to the interface, and λ_S is the spin diffusion length in the neatly deposited OSE sub-layer. The spin polarization p is defined

as the ability of the FM electrode to inject carriers with aligned spins. We express the thickness dependence of the GMR magnitude, *ΔR/R*, which is the maximum relative change in electrical resistance, *R* within the spin-valve hysteresis loop, assuming no loss of spin memory at the interfaces due to the self-adjusting capability of the OSE [11] using Eq.(1) as given below [12]

$$\frac{\Delta R}{R} = \frac{R_{AP} - R_P}{R_{AP}} = \frac{2 p_1 p_2 e^{-(d-d_0)/\lambda_s}}{1 + p_1 p_2 e^{-(d-d_0)/\lambda_s}}$$

where R_{AP} and R_P denote *R* in the anti-parallel and parallel magnetization configurations, respectively, and (d-d_0) is the thickness of the neatly deposited OSE sub-layer. For inverse magnetoresistance, $R_{AP} < R_P$; therefore *ΔR/R* is negative according to Eq. (1). We used Eq. (1) with three adjustable parameters, namely p_1p_2, d_0 and λ_S to fit the data for *ΔR/R* in Fig. 2b. The good agreement shown in Fig. 2b was obtained with the following parameters: p_1p_2 = -0.32; d_0 = 87 nm, which is close to the lower limit of d below which the I-V response becomes linear; and λ_S = 45 nm, which is a reasonable value for the spin diffusion length in the neatly deposited OSE sub-layer. The obtained λ_S is smaller than what was extracted for T_6 (ref. 12), possibly due to the aluminium element in Alq_3 that may increase the spin-orbit coupling in this OSE. However, λ_S is similar to what was extracted from spin valve devices of single-walled carbon nanotubes.

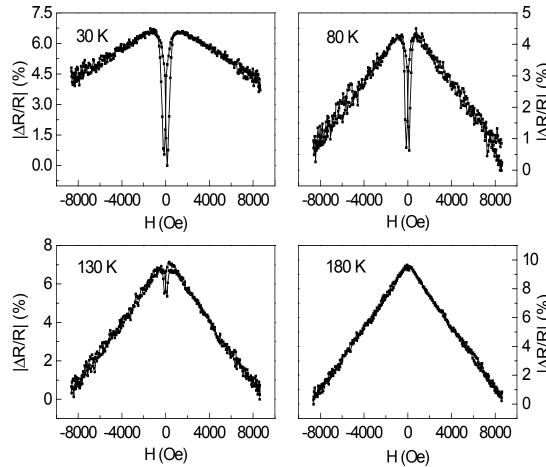

FIGURE 3. The magnetoresistance response of the device in Fig. 2a at different temperatures from 30 K to 180 K.

We measured the dependences of *ΔR/R* of the organic spin-valve devices on the applied bias voltage, V and temperature, T. We found that *ΔR/R* is in fact asymmetric with the bias V; the reason for that is not clear at the present time. *ΔR/R* also strongly depends on the temperature, T. A series of GMR hysteresis is shown in Fig. 3. The spin-valve effect diminishes with T and actually disappears at T = 180 K. The temperature dependence of

ΔR/R does not qualitatively follow that of the magnetization of the LSMO itself; *ΔR/R* vanishes at $T < T_c$ of the LSMO (~ 300 K). We conclude that the spin-valve decrease is due to the decrease of λ_S with T, which has a stronger T dependence than that of the LSMO magnetization.

At elevated temperatures we found an additional interesting effect; an increase in high-field magnetoresistance (HFMR) accompanies the decrease of the low-field spin-valve related GMR (Fig. 3). We have also observed a similar but much smaller HFMR in the LSMO film itself. However the spin-valve device resistance is several orders of magnitude greater than that of the LSMO electrode. Therefore, the HFMR cannot be simply explained by the change in the serial resistance of the LSMO electrode. We found similar HFMR response in other two-terminal devices using LSMO electrodes [15] where the opposite electrode was not magnetic. We conclude therefore that the HFMR occurs at the LSMO/OSEC interface, and is probably due to the shift of the LSMO Fermi level with *H*. This model can also explain the recently measured room temperature resistance difference between two magnetic fields in planar LSMO/T_6/LSMO devices [16]. In that device it was claimed that spins injection and spin transport at room temperature was proven. This was a premature claim, since a simple MR at the LSMO/OSEC interface could explain the results. The spin diffusion within the OSEC, however diminishes at room temperature, as we concluded above.

In conclusion, the present study shows that spin-polarized carrier injection, transport and detection, which are the main ingredients of Spintronics, can be successfully achieved using π-conjugated OSE. This may initiate a variety of exciting new applications in organic Spintronics such as spin-OLEDs, enabled by the novel functionalities of the OSEC. This is therefore the debut of Organic Spintronics.

ACKNOWLEDGMENTS

This work was funded in part by the DOE grants # 04-ER-46109 and 04-ER-46161.

REFERENCES

1. Baibich, M. N. et al., *Phys. Rev. Lett.* 61, 2472-2475 (1988).
2. Wolf, S. A. et al., *Science* 294, 1488-1490 (2001).
3. Daughton, J., *J. Magn. Mat*. 192, 334-338 (1999).
4. Johnson, M., and Silsbee, R. H., *Phys. Rev. Lett*. 55, 1790-1793 (1985).
5. Merservey, M. and Tedrow, P. M., *Phys. Rep*. 238, 173 (1994).
6. Schmidt, G. et al., *Phys. Rev. B* 62, R4790-4793 (2000).
7. Rashba, E. I., *Phys. Rev. B* 62, R16267-16270 (2000).
8. Smith, D. L., and R. N. Silver, Phys. Rev. B 64, 045323 (2001).
9. Albrecht, J. D., and Smith, D. L., *Phys. Rev. B* 66, 113303 (2002).
10. Bassler, H., *Polym. Adv. Technol*. 9, 402 (1998).
11. Ruden, P. P., and Smith, D. L., *J. Appl. Phys*. 95, 4898-4903 (2004).
12. Xiong, Z. H., Wu, D., Vardeny, Z. V., and Shi, J. *Nature* 427, 821-824 (2004).
13. Hwang, H. Y. et al., *Phys. Rev. Lett.* 77, 2041-2044 (1996).
14. Ramirez, A. P., *J. Phys.: Cond. Mat.* 9, 8171 (1997).
15. Wu, D., Xiong, Z. H., Vardeny, Z. V., and Shi, J., *Phys. Rev. Lett.* (in press).
16. V. Dediu, V., Murgia, M., Matacotta, F. C., Taliani, C., and Barbanera, S., *Solid State Commun*. 122, 181-184 (2002).

Copyright of AIP Conference Proceedings is the property of American Institute of Physics. The copyright in an individual article may be maintained by the author in certain cases. Content may not be copied or emailed to multiple sites or posted to a listserv without the copyright holder's express written permission. However, users may print, download, or email articles for individual use.